Chinese Science Bulletin

An acetylcholinesterase inhibitor, 3-benzidino-5-methyl-6-phenylpyridazine, blocking outward potassium currents in acutely isolated rat hippocampal pyramidal neurons

DU HuiZhi, LI MiaoYu & YANG Pin†

Key Laboratory of Chemical Biology and Molecular Engineering of Ministry of Education, Institute of Molecular Science, Shanxi University, Taiyuan 030006, China

3-benzidino-5-methyl-6-phenylpyridazine (BMP) inhibited electric eel acetylcholinesterase (AChE), with IC_{50} being 0.58 μmol·L^{-1}. As an AChE inhibitor, the effects of BMP on delayed rectifier potassium current ($I_{K(DR)}$) and transient outward potassium current ($I_{K(A)}$) in acutely isolated rat hippocampal pyramidal neurons were studied using the whole cell patch-clamp technique. BMP (0.1—50 μmol·L^{-1}) inhibited $I_{K(DR)}$ and $I_{K(A)}$ in a concentration-dependent and voltage-independent manner. The IC_{50} value for the blocking action of BMP on $I_{K(DR)}$ and $I_{K(A)}$ was calculated to be 2.92 and 2.11 μmol·L^{-1}, respectively. At the concentration of 10 μmol·L^{-1}, BMP shifted the activation curve of IK(DR) to negative potential by 8.85 mV. Meanwhile, at the concentration of 10 μmol·L^{-1}, BMP also shifted the activation and the steady-state inactivation curve of $IK_{(A)}$ to negative potential by 5.82 mV and 10.02 mV, respectively. In conclusion, BMP potently inhibits $I_{K(DR)}$ and $I_{K(A)}$ in rat hippocampal pyramidal neurons, which may contribute to restore the damaged central nervous system.

whole cell patch-clamp technique, hippocampal pyramidal neurons, 3-benzidino-5-methyl-6-phenylpyridazine, outward potassium currents

Alzheimer's disease (AD), the most common cause of dementia in the elderly, is a chronic, slowly progressive neurodegenerative disorder with characteristic deterioration of intellectual capacity in various domains: learning and memory, language abilities, reading and writing, praxis, and interaction with the environment[1]. It was hypothesized that the cognitive loss associated with AD was related to reduction of acetylcholine (ACh) and central cholinergic deficit. Thus, increasing ACh amounts by acetylcholinesterase (AChE) inhibitors might enhance cognitive function in AD patients[2,3].

Hippocampal neurons are the most important region for learning and memory in brain. Biological membranes are essential in maintaining cell integrity and function. Ion channels in cell membrane are targets for many toxins and drugs. Much medical damage or mend to the central nervous system (CNS) is achieved through medical disturbance of the function of ion channels[4,5]. There are many kinds of ion channels in rat hippocampal neurons, such as potassium channels, calcium channels and sodium channels. Potassium channels play a crucial role in regulating the electrical excitability of animal cells, being primarily responsible for the depolarization phase of the action potential. Furthermore, these potassium channels play important roles in regulation of learning and memory[6,7]. Enhancement of outward po-

Received July 25, 2008; accepted October 30, 2008
doi: 10.1007/s11434-008-0569-x
†Corresponding author (email: yangpin@sxu.edu.cn)
Supported by National Natural Science Foundation of China (Grant No. 20637010)

tassium current may participate in cortical neuronal death in AD[8]. Several AChE inhibitors were found to have effect on outward potassium currents in neurons. Tetrahydroaminoacridine (tacrine) inhibits delayed rectifier potassium current ($I_{K(DR)}$)[9,10] and transient outward potassium current ($I_{K(A)}$)[11]. Metrifonate inhibits slow component of the afterhyperpolarization tail current (sI_{AHP})[12]. Galantamine blocks $I_{K(DR)}$, but not $I_{K(A)}$ in rat dissociated hippocampal pyramidal neurons[13]. Donepezil blocks $I_{K(DR)}$ in pyramidal neurons of rat hippocampus and neocortex[14].

3-[(β-morpholinoethyl)amino]-4-methyl-6-phenylpyridazine dihydrochloride (minaprine, Figure 1) has selective affinity for muscarinc M1 receptors and possesses related memory-enhancing properties[15,16]. Also, it enhances short-term retention in rats in the social memory test[17]. A classical structure-activity relationship exploration suggests that the critical elements for high AChE inhibition are as follows: (i) presence of a central pyridazine ring, (ii) necessity of a lipophilic cationic head, and (iii) change from a 2- to a 4-5-carbon units distance between the pyridazine ring and the cationic head[18]. Recently, we have found that 3-benzidino-6(4-chlorophenyl) pyridazine (BCP) (Figure 1), we firstly synthesized in our laboratory, potently inhibited $I_{K(DR)}$ and $I_{K(A)}$ in a concentration-dependent and voltage-dependent manner in acutely isolated rat hippocampal pyramidal neurons by using whole cell patch-clamp technique[19]. Other groups associated with the pyridazine ring play a crucial role in the inhibition effect of the compound on the outward potassium currents, and might make the compound more specific for either $I_{K(DR)}$ or $I_{K(A)}$. Further studies involving other pharmacological compounds structurally related to BCP or minaprine are needed to understand the roles of various groups in the blockade of the potassium currents. Then, using pyridazine and benzidine as building blocks, we synthesized 3-benzidino-5-methyl-6-phenylpyridazine (BMP, Figure 1), which has IC_{50} of 0.58 μmol·L^{-1} on electric eel AChE. In the present study, we investigated the effects of BMP on outward potassium currents including $I_{K(DR)}$ and $I_{K(A)}$ in acutely isolated rat hippocampal pyramidal neurons.

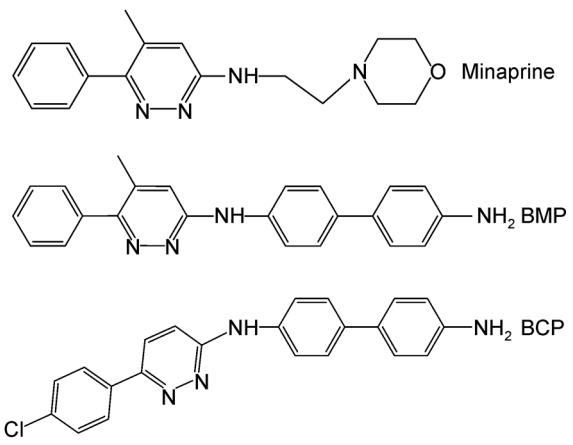

Figure 1 Structrues of minaprine, BCP and BMP.

1 Materials and method

1.1 Isolation of single rat hippocampal pyramidal neurons

Single rat hippocampal pyramidal neurons were acutely isolated by enzymatic digestion and mechanical dispersion[19]. Wistar rats of 7—10 days were purchased from the Experimental Animal Center of Shanxi Medical University (Grade II, Certificate No. 070101). All experiments conformed to local and international guidelines on ethical use of animals and all efforts were made to minimize the number of animals used and suffering. Briefly, 400–600 μm thick brain slices were cut from hippocampal region in ice-cold artificial cerebrospinal solution (ACS). These tissue pieces were incubated for at least 30 min at 32℃ in ACS, and then transferred into ACS containing 0.5 mg/ml protease at 32℃ for 35 min. Throughout the entire procedure, the media were continuously saturated with a 95%O_2—5%CO_2 gas to maintain a pH value of 7.4. After digestion, the tissue pieces were washed 3 times with ACS. Through a series of Pasteur pipettes with decreasing tip diameter, neurons were isolated by triturating the brain fragments. Then, the cell suspension was maintained at room temperature in extracellular solution before the electrophysiological experiment. All experiments were performed within 6 h after isolation.

1.2 Potassium currents' recording technique

The cell suspension was transferred into an experimental chamber mounted on the stage of an inverted microscope (Chongqing, China) with 1 ml extracellular solution. After 20 min, pyramidal cells settled on the bottom of the chamber. $I_{K(DR)}$ and $I_{K(A)}$ currents were recorded with an Axopatch 200B patch clamp amplifier (Axon Instruments, Foster City, CA, USA). Glass microelectrodes were made using micropipette puller (PP 830, Narishige, Japan) and had a resistance of 7—12 MΩ when filled with electrode internal solution. Neurons

with bright, smooth appearance and apical dendrites were selected for recording. Liquid junction potential between the pipette solution and external solution was corrected after the pipette tipped into the external solution. After forming a conventional "gigaseal", the membrane was ruptured with a gentle suction to obtain the whole cell voltage clamp. To minimize the duration of capacitive current, membrane capacitance and series resistance were compensated after membrane rupture. Evoked currents were low-pass filtered at 2 kHz, and digitized at 10 kHz, and command pulses were generated by a Digidata 1200B (Axon) controlled by pCLAMP version 6.0.4 software (Axon Instruments, CA, USA), and on-line acquired data stored in a PC486 computer for subsequent analysis. All experiments were carried out at room temperature (20℃—26℃).

1.3 Preparation of experimental solutions (mmol·L^{-1})

Artificial cerebrospinal solution (ACS): NaCl 124, KCl 5, KH_2PO_4 1.2, $MgSO_4$ 1.3, $CaCl_2$ 2.4, Glucose 10, $NaHCO_3$ 26, pH 7.4. Extracellular solution: NaCl 150, KCl 5, $MgCl_2$ 1.1, $CaCl_2$ 2.6, Glucose 10, *N*-[2-hydroxyethyl]-piperazine-*N*'-[2-ethanesulfonic acid] (HEPES) 10, pH 7.4. To record potassium current, 1 μM tetrodotoxin (TTX) and 0.2 mM $CdCl_2$ were added to extracellular solution before the electrophysiological recording. Electrode internal solution: KCl 65, KOH 5, KF 80, $MgCl_2$ 2, HEPES 10, ethylene glycol-bic[2-aminoethylether]*N*,*N*,*N*′,*N*′-tetraacetic acid (EGTA) 10, adenosine triphosphate disodium salt (Na_2ATP) 2, pH 7.3.

1.4 Data analysis

All data were analyzed by the use of pCLAMP 6.0 and Origin 5.0 software (Microcal software, USA). All values were presented as mean ± S.D., and statistical comparisons were made using the paired Student's t test and one-way ANOVA procedure, and the probabilities less than 0.05 were considered significant.

2 Results

2.1 Separation of $I_{K(DR)}$ and $I_{K(A)}$

In whole cell patch-clamp recording, the total potassium currents were recorded with 150 ms depolarizing pulses from −50 to +60 mV in 10 mV steps following a hyperpolarizing prepulse of 400 ms to −110 mV (Figure 2(a)). The delayed rectifier potassium currents ($I_{K(DR)}$) were elicited by a similar protocol in which a 50 ms interval at −50 mV was inserted after the prepulse. Currents at the end of the depolarizing pulse were referred to as $I_{K(DR)}$ (Figure 2(b)). Subtraction of Figure 2(a) from Figure 2(b) revealed the fast transient potassium currents ($I_{K(A)}$). The peak of the subtracted currents was referred to as $I_{K(A)}$ (Figure 2(c)).

Effects of BMP on $I_{K(DR)}$ or $I_{K(A)}$ were observed at +60 mV when depolarized from −50 mV. In the control test without BMP, $I_{K(DR)}$ and $I_{K(A)}$ decreased by 3.5 ± 2.1% and 4.2 ± 3.0% (n = 8) in 15 min current-recording, respectively. Upon the application of BMP (10 μmol·L^{-1}), the inhibitory effect of BMP on $I_{K(DR)}$ occurred in a few minutes until reached a maximum and

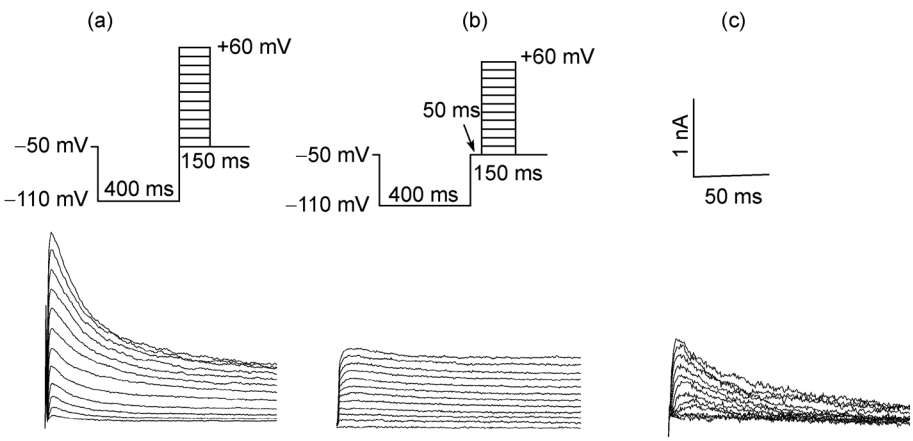

Figure 2 Outward potassium currents in a hippocampal pyramidal neuron. (a) Total outward potassium current stimulated with 150 ms depolarizing pulses from −50 to +60 mV in 10 mV steps following a hyperpolarizing prepulse of 400 ms to −110 mV (inset). (b) $I_{K(DR)}$ stimulated with similar protocol in (a), except for a 50 ms interval at −50 mV inserted after the prepulse (inset). (c) Isolated $I_{K(A)}$ by subtracting current traces of (b) from those of (a).

steady value in about 12 min (data not shown). With different concentration of BMP, it took 12 ± 2 min for inhibitory effects on $I_{K(DR)}$ and $I_{K(A)}$ to reach the steady value. Therefore, in the present study, signals were firstly recorded in natural state, and then recorded in 12 min after addition of BMP into external solution.

2.2 BMP-decreased $I_{K(DR)}$ and $I_{K(A)}$ in a concentration-dependent manner

Upon the application of BMP, the amplitudes of $I_{K(DR)}$ and $I_{K(A)}$ decreased, and this action progressed with increment in concentrations from 0.1 to 50 μmol·L^{-1} (including: 0.1, 0.5, 1, 5, 10 and 50 μmol·L^{-1}, respectively). Concentration-response curve was obtained by plotting the inhibition percentage against the concentration of BMP (Figure 3(a)), and the curve was fitted with the Hill function: $I=I_{max}/[1+(IC_{50}/C)^n]$, where I is the percent inhibition, I_{max} is the maximal percent inhibition, IC_{50} is 50% of maximum inhibition, C is the concentration of BMP, and n is the Hill coefficient. The IC_{50} value of BMP for blocking $I_{K(DR)}$ was calculated to be 2.92 ± 0.81 μmol·L^{-1} with n of 0.99 ± 0.24, and the IC_{50} value of BMP for blocking $I_{K(A)}$ was calculated to be 2.11 ± 0.44 μmol·L^{-1} with n of 0.82 ± 0.13. The result indicated that BMP decreased $I_{K(DR)}$ and $I_{K(A)}$ in a concentration-dependent manner.

2.3 Effects of BMP on current-voltage relationships of $I_{K(DR)}$ and $I_{K(A)}$

Figure 3(b) shows current-voltage (I-V) curves of $I_{K(DR)}$ and $I_{K(A)}$ generated by depolarizing steps from a holding potential of −50 mV to +60 mV with a 10 mV increment. In the presence of 10 μmol·L^{-1} BMP, the amplitude of $I_{K(DR)}$ and $I_{K(A)}$ was significantly decreased at the test potentials between 20 mV and 60 mV (n = 6, $P < 0.01$). The percent inhibition of $I_{K(DR)}$ and $I_{K(A)}$ upon BMP application was not a function of the depolarizing potential (Figure 3(c)), indicating that BMP does not sense the electric field in the pore.

2.4 Effects of BMP on activation of $I_{K(DR)}$ and $I_{K(A)}$

Effects of BMP on activation of $I_{K(DR)}$ and $I_{K(A)}$ were detected by conductance-voltage relationship. $I_{K(DR)}$ and $I_{K(A)}$ are recorded in Figure 2. The activation curves for $I_{K(DR)}$ and $I_{K(A)}$ in the absence and presence of 10 μmol·L^{-1} BMP are shown in Figure 3(d). Conductance-voltage curves were constructed by plotting G/G_{max} vs. membrane potentials, and the curves were fitted by a Boltzmann equation: $G/G_{max}=1/\{1+\exp[-(V-V_{1/2})/k]\}$, where G is conductance, G_{max} is maximum conductance, V is membrane potential, $V_{1/2}$ is the potential for half-maximal activation, and k is the slope factor; Conductance was calculated by using the equation: $G=I/(V-V_K)$, where I is current amplitude, V is membrane potential and V_K is the reversal potential. In the absence and presence of 10 μmol·L^{-1} BMP, the value of $V_{1/2}$ was (3.54 ± 0.84) and (–5.31 ± 1.20) mV (n = 5, $P < 0.01$), with k of (21.24 ± 2.37) and (21.48 ± 1.36) mV (n = 5, $P > 0.05$) for $I_{K(DR)}$ and the value of $V_{1/2}$ was (10.60 ± 0.87) and (4.78 ± 1.60) mV (n = 5, $P < 0.01$), with k of (19.82 ± 1.25) and (18.91 ± 1.93) mV (n = 5, $P > 0.05$) for $I_{K(A)}$. BMP (10 μmol·L^{-1}) caused a negative shift of the activation curve of $I_{K(DR)}$ and $I_{K(A)}$ along the potential axis. However, the slope factor k remained unchanged.

2.5 Effects of BMP on steady-state inactivation of $I_{K(A)}$

Figure 4 shows the effect of BMP on the voltage-dependence of $I_{K(A)}$ inactivation using a double-pulse protocol: currents were elicited with a 120 ms test pulse to +60 mV preceded by 80 ms prepulses to potentials between −120 and −10 mV, and holding potential is −100 mV. The steady-state inactivation curves were obtained by plotting the normalized $I_{K(A)}$ against the prepulse voltages. The plots were well fitted with a single Boltzmann function: $I/I_{max}=1\{1+\exp[(V-V_{1/2})/k]\}$, where I/I_{max} is the normalized data, V is the prepulse potential, $V_{1/2}$ is the potential where normalized I was reduced to one half and k is the slope factor. In the absence and presence of 10 μM BMP, the value of $V_{1/2}$ was (–30.71 ± 1.17) mV and (–40.73 ± 0.54) mV (n = 5, $P < 0.01$), with k of (–7.40 ± 1.02) mV and (–9.94 ± 0.26) mV(n = 5, $P > 0.05$). BMP (10 μmol·L^{-1}) caused a negative shift of the steady-state inactivation curve along the potential axis. However, the slope factor k remained unchanged.

2.6 Effects of BMP on kinetics of $I_{K(DR)}$ and $I_{K(A)}$ activation and inactivation

The time course of $I_{K(A)}$, including its fast activation time and rapid inactivation time, was analyzed, and the effects of BMP on the time course of $I_{K(A)}$ were studied. BMP did not affect the time to reach the peak of $I_{K(A)}$ and the activation of $I_{K(A)}$ (Figure 5(a)). In the absence of BMP, having been evoked by 60 mV depolarizing pulse from the holding potential of −50 mV, $I_{K(A)}$

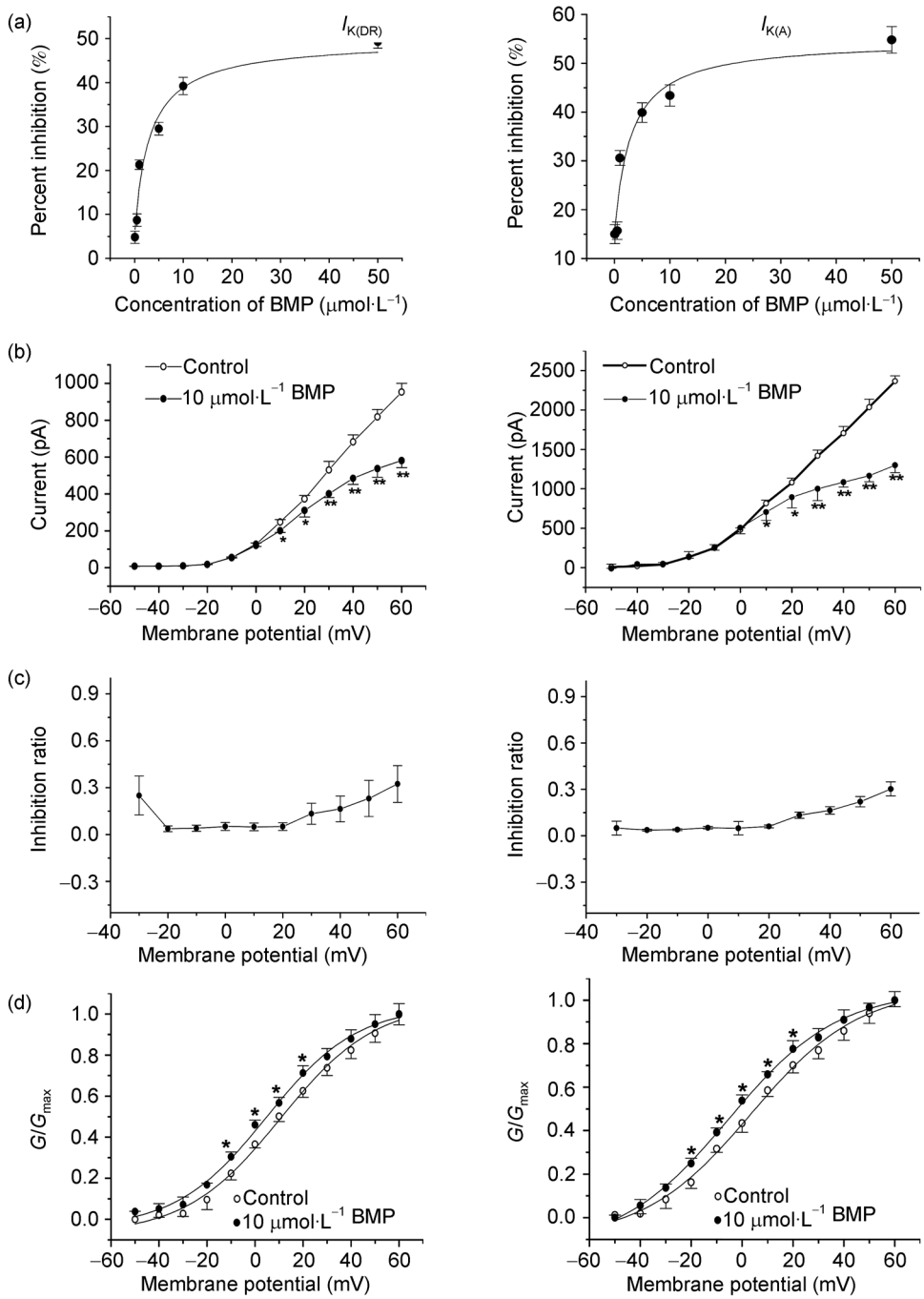

Figure 3 Effects of 10 μmol·L^{-1} BMP on $I_{K(DR)}$ (left) and $I_{K(A)}$ (right). *P < 0.05, **P < 0.01 vs. control. Each point represents mean of five cells. (a) Concentration-response curves for the blockade of BMP on $I_{K(DR)}$ and $I_{K(A)}$. (b) I-V curves of $I_{K(DR)}$ and $I_{K(A)}$ in the absence (○) and presence (●) of 10 μmol·L^{-1} BMP. (c) Percent inhibition in $I_{K(DR)}$ and $I_{K(A)}$ caused by 10 μmol·L^{-1} BMP application as a function of depolarizing potentials. The percent inhibition of $I_{K(DR)}$ and $I_{K(A)}$ upon BMP application was not a function of the depolarizing potential. (d) Activation curves of $I_{K(DR)}$ and $I_{K(A)}$ in the absence (○) and presence (●) of 10 μmol·L^{-1} BMP. The data were well fitted by Boltzmann equation.

reached maximal peak by 3.58 ± 0.20 ms after stimulation. After extracellular application of 10 μmol·L^{-1} BMP, the activation time of $I_{K(A)}$ significantly decreased to 3.00 ± 0.10 ms (n = 5, P > 0.05). BMP shortened the rapid inactivation time of $I_{K(A)}$ and accelerated the inactivation of $I_{K(A)}$ in a concentration-dependent manner (Figure 5(b)). The rapid inactivation time of $I_{K(A)}$ was 64.20 ± 1.20 ms, and significantly decreased to 40.20 ± 1.10 ms by extracellular application of 10 μmol·L^{-1} BMP (n = 5, P < 0.01).

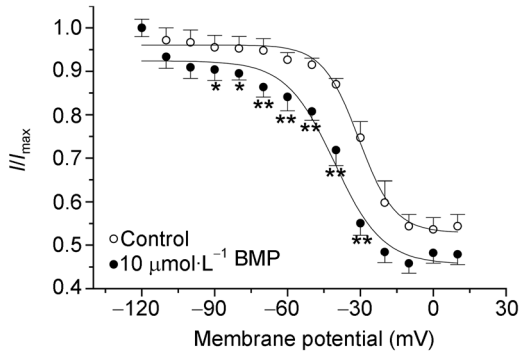

Figure 4 Effects of BMP on steady-state inactivation of $I_{K(A)}$. Normalized steady-state inactivation curves of $I_{K(A)}$ in the absence (○) and presence (●) of 10 μmol·L^{-1} BMP were plotted as a function of the conditioning voltages and fitted with Boltzmann function. The value of each point is mean of five cells. *P < 0.05, **P < 0.01 vs. control.

The slow activation time course of $I_{K(D)}$ was analyzed, and the effects of BMP on the time course of $I_{K(A)}$ were studied. In the absence of BMP, $I_{K(D)}$ reached a maximum and steady value of 28.30 ± 1.20 ms. After extracellular application of 10 μmol·L^{-1} BMP, the activation time of $I_{K(D)}$ significantly increased to 27.40 ± 0.61 ms (n = 5, P > 0.05). BMP (0.1—50 μmol·L^{-1}) did not affect the time to reach a maximum and steady value of $I_{K(D)}$ and the activation of $I_{K(D)}$ (Figure 5(c)).

3 Discussion

Minaprine, besides its original antidepressive properties, has cholinomimetic activities that could be, at least in part, mediated by their selective affinity for M1 muscarinic receptors. An *in vivo* administration of minaprine (30 mg/kg) to rats significantly increases ACh levels in the hippocampus (38%). While, minaprine presents a very weak *in vitro* activity on electric eel AChE (IC_{50} = 600 μmol·L^{-1})[18,20]. Thus, minaprine may be developed into a potential remedy for the treatment of senile dementias and cognitive impairments occurring in elderly people. The main acting group of minaprine is pyridazine ring[16]. Using pyridazine and benzidine as building blocks, we obtained two novel compounds (including BCP and BMP). These two compounds have a central pyridazine ring in common with minaprine. We investigated the effects of them on electric eel AChE. BCP and BMP inhibited electric eel AChE as an inhibitor (IC_{50} = 0.30 and 0.58 μmol·L^{-1}, respectively), with an increased potency being 1000—2000 times

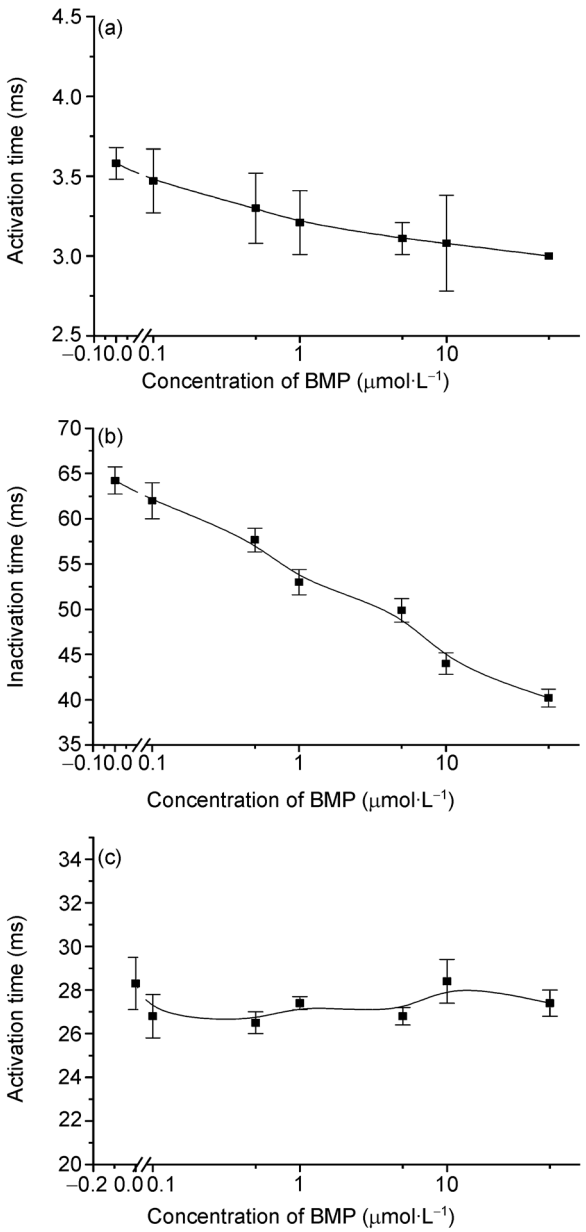

Figure 5 Effects of BMP on kinetics of $I_{K(A)}$ and $I_{K(D)}$ activation and inactivation. (a) BMP did not affect the time to reach the peak of $I_{K(A)}$ and the activation of $I_{K(A)}$ (n = 5, P > 0.05). (b) BMP shortened the rapid inactivation time of $I_{K(A)}$ and accelerated the inactivation of $I_{K(A)}$ in a concentration-dependent manner (n = 5, P < 0.01). (c) BMP did not affect the time to reach a maximum and steady value of $I_{K(D)}$ and the activation of $I_{K(D)}$ (n = 5, P > 0.05).

greater than minaprine. The pyridazine and benzidine group of these two compounds maybe reacts with binding site of the binding pocket in electric eel AChE. In addition, the hydrogen-bonding interaction between these two compounds and electric eel AChE seems to play an important role[21]. When there is a substituting group in the 6-phenyl of the pyridazine ring or in the

5-position of the pyridazine ring, the inhibitory activities against electric eel AChE *in vitro* were different. Perhaps the substituent changed the electron density of the compound and changed its interaction with the active sites of AChE.

BCP (0.01—500 μmol·L^{-1}) inhibited $I_{K(DR)}$ and $I_{K(A)}$ in a concentration-dependent and voltage-dependent manner (IC_{50} = 7.13 and 0.55 μmol·L^{-1}, respectively). BCP (10 μmol·L^{-1}) shifted the activation curve of $I_{K(DR)}$ to positive potential by 29.09 mV, while shifting the activation and inactivation curve of $I_{K(A)}$ to positive potential by 34.18 mV and 22.47 mV, respectively[19]. In this study, we found that BMP inhibited $I_{K(DR)}$ and $I_{K(A)}$ in a concentration-dependent and voltage-independent manner (IC_{50} = 2.92 and 2.11 μmol·L^{-1}, respectively). At the concentration of 10 μmol·L^{-1}, BMP shifted the activation curve of $I_{K(DR)}$ to negative potential by 8.85 mV. Meanwhile, at the concentration of 10 μmol·L^{-1}, BMP also shifted the activation and the steady-state inactivation curve of $I_{K(A)}$ to negative potential by 5.82 mV and 10.02 mV, respectively. A substituting group in the 6-phenyl of the pyridazine ring or in the 5-position of the pyridazine ring in compounds weakens the inhibition effects of these compounds on outward potassium currents in acutely isolated rat hippocampal pyramidal neurons. But the sensitivity is different in these substituting groups to inhomogeneous outward potassium currents. The effects of BMP and BCP on $I_{K(DR)}$ and $I_{K(A)}$ are not the same. Therefore, the presence of other groups associated with the pyridazine ring might make the compound more specific for either $I_{K(DR)}$ or $I_{K(A)}$.

Several AChE inhibitors have been found effective on outward potassium currents in neurons. Tetrahydroaminoacridine (tacrine) inhibits $I_{K(DR)}$[9,10] and $I_{K(A)}$[11]. Galantamine blocks $I_{K(DR)}$, other than $I_{K(A)}$ in rat-dissociated hippocampal pyramidal neurons[13]. Donepezil blocks $I_{K(DR)}$ in pyramidal neurons of rat hippocampus and neocortex[14]. These studies differed in three important aspects that displayed in species (mouse vs. rat), cell types (cortical neurons vs. hippocampal neurons) and different approaches to get cells (cultured neuron cell vs. acutely isolated neuron cell). So the results were not identical. In addition, although tacrine is structurally related to the potassium channel blocker 4-aminopyridine (4-AP), the blockade of potassium channel by tacrine cannot be only attributed to the 4-AP-sensitive $I_{K(A)}$[9]. Further studies involving other pharmacological compounds structurally related to 4-AP and minaprine are needed to understand the role of various groups and structure-activity relationship of AChE inhibitors in the blockade of the potassium current[22]. Some systemization of new compounds and study of effects of BMP on other currents remain in progress.

Under physiological conditions, potassium currents are important for the regulation of neuronal excitability and the maintenance of baseline membrane potential. Potassium currents control action potential duration and repolarization, release of neurotransmitters and hormones, and Ca^{2+}-dependent synaptic plasticity. Since $I_{K(A)}$ is transient, repolarization is mainly related to $I_{K(DR)}$. As in other neurons, $I_{K(A)}$ in hippocampal neurons was thought to modulate the timing of repetitive action potential generation and the time required to reach the threshold to fire an action potential[23]. Enhancement of potassium currents leads to a reduction in $[K^+]_i$, involving the pathogenesis of neuronal death[24]. We also notice that the maximum inhibition of these two novel compounds (including BCP and BMP) on $I_{K(DR)}$ and $I_{K(A)}$ only reaches about 50% even at the maximum concentration. Because voltage-activated K^+ channels in rat pyramidal neurons are composed of various K^+ channel subtypes such as Kv1, Kv2, Kv3 and Kv4, these two compounds are probably selective to some K^+ channel subtypes[13]. It needs further studies to understand the channel selectivity of these two compounds.

The mechanism by which AChE inhibitors affect hippocampal potassium channels are not fully understood at this time. There are several potential interpretations. One is the electrostatic interactions between BMP and potassium channel proteins. In our study, BMP (10 μM) decreased the amplitudes of $I_{K(DR)}$ and $I_{K(A)}$ in voltage-independent manner, namely, the fractional reduction in $I_{K(DR)}$ and $I_{K(A)}$ upon BMP application was unaffected by changes in the depolarizing potential, indicating that BMP does not sense the electric field in the pore, coming in the vicinity of the selectivity filter of potassium channel. Therefore, if BMP blocks outward potassium channels via binding channel proteins, it likely binds an external site rather than inserting into the pore. Furthermore, the inhibition effects of BMP on outward potassium currents were obvious only at potentials more positive than 0 mV. These effects could be attributed to electrostatic interaction of BMP with the membrane[25]. Another possible mechanism might involve changes in membrane fluidity. Previous studies

have indicated that membrane fluidity is altered in central and peripheral cell systems in AD[26]. BMP seems to have more pronounced effects on membrane integrity and fluidity, which invests BMP with the property of protecting neuron. But, BCP inhibited $I_{K(DR)}$ and $I_{K(A)}$ in a voltage-dependent manner, so the mechanism by which it affects hippocampal potassium channels is possibly the electrostatic interactions between it and potassium channel proteins.

Our results support the proposition that the action of AChE inhibitors may be related to potassium channels[6]. The IC_{50} value of BCP and BMP towards $I_{K(DR)}$ and $I_{K(A)}$ in this study is slightly greater than that towards AChE on electric eel. It suggests that these two compounds appear to be more sensitive to AChE than to the two kinds of currents and AChE could be major action site of them. However, potassium channels might still be other new targets for AChE inhibitors besides AChE. Also it would be more significant once research targets are expanded to other mammalian neurons.

1 Tariot P N. Alzheimer's disease: An overview. Alzheimer Dis Assoc Dis, 1994, 8: S4—S11[DOI]
2 Benzi G, Moretti A. Is there a rationale for the use of acetylcholinesterase inhibitors in the therapy of Alzheimer's disease? Eur J Pharmacol, 1998, 346: 1—13[DOI]
3 Mega M S. The cholinergic deficit in Alzheimer's disease: Impact on cognition, behaviour and function. Int J Neuropsychopharmacol, 2000, 3: 3—12[DOI]
4 Taylor C P, Meldrum B S. Na^+ channels as targets for neuroprotective drugs. Trends Pharmacol Sci, 1995, 16: 309—316[DOI]
5 Calavresi P, Pisani A, Mercuri N B, et al. On the mechanisms underlying hypoxia-induced membrane depolarization in striatal neurons. Brain, 1995, 118: 1027—1038[DOI]
6 Harvey A L, Rowan E G. Effects of tacrine, aminopyridines, and physostigmine on acetylcholinesterase, acetylcholine release, and potassium currents. Adv Neurol, 1990, 51: 227—233
7 Landifield P W, Pilter T A. Prolonged Ca^{2+}-dependent after hyperpolarizations in hippocampal neurons of aged rats. Science, 1984, 226: 1089—1095[DOI]
8 Yu S P, Farhangrazi Z S, Ying H S, et al. Enhancement of outward potassium current may participate in β-amyloid peptide-induced cortical neuronal death. Neurobiol Disease, 1998, 5: 81—88[DOI]
9 Kraliz D, Singh S. Selective blockade of the delayed rectifier potassium current by tacrine in Drosophila. J Neurobiol, 1997, 32: 1—10[DOI]
10 Zhang W, Jin H W, Xu S F, et al. Inhibition of tacrine on delayed rectifier and transient outward potassium currents in cultured rat hippocampal neurons. Acta Pharm Sin, 2004, 39: 93—96
11 Rogawski M A. Tetrahydroaminoacridine blocks voltage-dependent ion channels in hippocampal neurons. Eur J Pharmacol, 1987, 142: 169—172[DOI]
12 Power J M, Oh M M, Disterhoft J F. Metrifonate decreases sIAHP in CA1 pyramidal neurons *in vitro*. J Neurophysiol, 2001, 85: 319—322
13 Pan Y P, Xu X H, Wang X L. Galantamine blocks delayed rectifier, but not transient outward potassium current in rat dissociated hippocampal pyramidal neurons. Neurosci Lett, 2002, 336: 37—40[DOI]
14 Zhong C B, Zhang W, Wang X L. Effects of donepezil on the delayed rectifier-like potassium current in pyramidal neurons of rat hippocampus and neocortex. Acta Pharm Sin, 2002, 37: 415—418
15 Sansone M, Battaglia M, Vetulani J. Minaprine, but not oxiracetam, prevents desipramine-induced impairment of avoidance learning in mice. Pol J Pharmacol, 1995, 47: 69—73
16 Worms P, Kan J P, Steinberg R, et al. Cholinomimetic activities of minaprine. Naunyn Schmiedebergs Arch Pharmacol, 1989, 3401: 411—418[DOI]
17 Puglisi-Allegra S, Cabib S, Cestari V, et al. Post-training minaprine enhances memory storage in mice: involvement of D1 and D2 dopamine receptors. Psychopharmacol, 1994, 113: 476—480[DOI]
18 Contreras J M, Rival Y M, Chayer S, et al. Aminopyridazines as acetylcholinesterase inhibitors. J Med Chem, 1999, 42: 730—741[DOI]
19 Du H Z, Zhang C F, Li M Y, et al. 3-benzidino-6 (4-chlorophenyl) pyridazine blocks delayed rectifier and transient outward potassium current in acutely isolated rat hippocampal pyramidal neurons. Neurosci Lett, 2006, 402: 159—163[DOI]
20 Garattini S, Forloni G L, Tirelli S, et al. Neurochemical effects of minaprine, a novel psychotropic drug, on the central cholinergic system of the rat. Psychopharmacol, 1984, 82: 210—214[DOI]
21 Sussman J L, Harel M, Frolow F, et al. Atomic structure of acetylcholinesterasefrom *Torpedo californica*: A prototypic acetylcholine-binding protein. Science, 1991, 253: 872—879[DOI]
22 Sugimoto H. Structure-activity relationships of acetylcholinesterase inhibitors: Donepezil hydrochloride for the treatment of Alzheimer's disease. Pure Appl Chem, 1999, 71: 2031—2037[DOI]
23 Gao B X, Ziskind-Conhaim L. Development of ionic currents underlying changes in action potential waveforms in rat spinal motoneurons. J Neurophysiol, 1998, 80: 3047—3061
24 Bortner C D, Hughes Jr. F M, Cidlowski J A. A primary role for K^+ and Na^+ efflux in the activation of apoptosis. J Biol Chem, 1997, 272: 32436—32442[DOI]
25 Zhang C F, Yang P. Zinc-induced aggregation of Aβ (10—21) potentiates its action on voltage-gated potassium channel. Biochem Biophys Res Commun, 2006, 345: 43—49[DOI]
26 Hajimohammadreza I, Brammer M J, Eagger S, et al. Platelet and erythrocyte membrane charges in Alzheimer's disease. Biochim Biophys Acta, 1990, 1025: 208—214[DOI]